Original scientific paper

NUMERICAL MODEL OF A LOCAL CONTACT OF A POLYMER NANOCOMPOSITE AND ITS EXPERIMENTAL VALIDATION

Andrey I. Dmitriev[1,2]

[1]Institute of Strength Physics and Materials Science SB RAS, Tomsk, Russia
[2]Tomsk State University, Tomsk, Russia

Abstract. *In the paper a model of a local contact of a polymer-based nanocomposite was developed within the method of a movable cellular automaton. The features of mechanical behavior of nanocomposite at the mesoscale level under dry sliding were studied with explicit account for the microprofile of the counterbody surface and the characteristic sizes of nanofiller. Factors that contribute to the conditions for the formation of a stable tribofilm of silica nanoparticles are analyzed. Two other parameters like sample geometry and the value of relative sliding velocity are also examined. It is shown that the thickness of tribofilm depends on stress conditions at the contact, and the friction coefficient decreases with increasing sliding velocity similar to one observed experimentally. To ensure the low friction properties of polymer nanocomposite, particles whose sizes are comparable with the characteristic size of the substrate microprofile are preferred. Results of numerical simulation are in good correlation with available experimental data.*

Key words: *Modelling, Nanocomposite, Silica nanoparticles, Carbon fibers, Tribofilm, Friction coefficient, Movable cellular automata method*

1. INTRODUCTION

Polymer matrix composites are the most significant class of composites finding widespread applications in almost all sectors of society and industry. These composites have increasingly been objects of an important topic of study due to the possibility of significant changes in their mechanical, physical, and other properties through the use of fillers of various types. In recent years, in the polymer nanocomposites (PNCs), along with traditional fillers, various nanosized particles added to the composite mixture have been becoming more widespread. The main advantage of these materials is characterized by the use of a low concentration of nanofiller (1–5% vol.) and by their particle size, in

contrast with conventional composites [1-4]. The size reduction from microscopic to nanoscopic scale indicates a dramatic increase in the interfacial area as compared with ordinary composites, resulting in an improvement in the material properties. Thus in [5], it was established that the wear rate of PNC based on polyphenylene sulfide decreased when TiO_2 and CuO particles were used as the fillers but increased with ZnO and SiC fillers. A noticeable increase in microhardness and fracture toughness of nanocomposite with nanosized inclusions is described in [6]. The effect of Young's modulus values increasing by almost 20% was found in [7] and an increase in the elastic modulus and yield stresses was shown in [8]. In [9] and [10], the effect of a significant change in the frictional performance of PNCs with the addition of carbon nanofibers and other nanoscale fillers was shown. Thus, the possibility of a targeted effect on the mechanical properties of a polymer-based nanocomposite makes them unique objects with the potential for widespread use in various modern applications.

As it was revealed in [11] the monodisperse silica nanoparticles (SNP) (diameter ~20 nm), produced via a sol-gel process, greatly improve the tribological behavior of conventional epoxy (EP, bisphenol A) composites when sliding against standard bearing steel (100Cr6). The monodisperse nanoparticles and the conventional fillers, e.g. short carbon fibers (SCF) and graphite, are beneficial with respect to desired tribological properties. It was shown earlier [10] that the tribological performance of such polymer composites can be significantly enhanced by the formation of a thin, well-distributed and load-carrying transfer film also called a tribofilm. With the addition of the nanoparticles, the friction coefficient drops very fast within the initial 1 hour, owing to the fast building up of a tribofilm. With enhancing the pressure from 1 to 3 MPa, the friction coefficient of the conventional composite becomes much higher. Opposite to the previous observation, the increase in pressure reduces the friction coefficient of polymer-based composite with SNP and SCF. Especially at high pv (the pressure multiplied by the sliding velocity) factors, nanoparticles reduce much more the wear than sub-micron particle combinations do (3 vol.% TiO_2/4 vol.%ZnS, diameter ~0.3 μm).

Although many publications have shown the importance of tribofilms during dry friction applications, only a few studies provide information about their structure. This is because these films are usually very thin and nanocrystalline that requires special tedious and expensive sample preparation techniques such as Focused Ion Beam (FIB) machining to characterize them with a Transmission Electron Microscope (TEM). A systematic study with changing the surface topography within the range of 0.01 to ~ 1 μm was performed by Zhang et al in [12]. They revealed that on very rough counterbody surfaces with Ra = ~1 μm two types of the transfer film could be identified. A carbon-based transfer film was formed in deeper grooves while the transfer film made from silica particles was identified in shallow grooves. Despite the progress made, a number of key questions, however, remain unanswered.

The aims of this work are the following. Firstly, to develop a numerical model of a local contact of PNC and to study the impact of filler properties and sample geometry on features of tribolayer formation. Secondly, to analyze the effect of pv-factor on tribological properties of hybrid PNC and to compare the numerical results with the available experimental data.

2. MODEL DESCRIPTION

A model of a local contact of polymer-based hybrid nanocomposite was developed within the method of the movable cellular automaton (MCA) [13-17]. In the MCA method the modeled objects are considered as a system of finite size bodies interacting with each other. In contrast to other particle-based approaches the MCA method uses the many-particle interaction where the force calculations are based on the spatial configuration of nearest neighbors. Within this approximation the system of Newton-Euler equations of motion will be written as follow [17]:

$$\begin{cases} m_i \dfrac{d^2 \vec{R}_i}{dt^2} = \vec{F}_i = \vec{F}_p^i + \vec{F}_v^i = \left(\sum_{j=1}^{N_i} \vec{F}_{pair}^{ij} + \vec{F}_\Omega^i \right) + \sum_{j=1}^{N_i} \left(\vec{F}_{nv}^{ij} + \vec{F}_{\tau v}^{ij} \right) \\ \hat{J}_i \dfrac{d^2 \vec{\theta}_i}{dt^2} = \sum_{j=1}^{N_i} \vec{M}_{ij} \end{cases} . \tag{1}$$

In Eq. (1) $\vec{R}_i$ and $\vec{\theta}_i$ are the radius-vector and rotation angle of the movable cellular automaton i, m_i and $\hat{J}_i$ are the particle mass and its moment of inertia, $\vec{F}_p^i$ and $\vec{F}_v^i$ are the potential and viscous constituents of the total force $\vec{F}_i$ acting on the automaton i, $\vec{M}_{ij}$ is the momentum of the total force, N_i is the number of neighboring particles for the automaton i. The potential force $\vec{F}_p^i$ is written as a sum of the pair-wise component $\vec{F}_{pair}^{ij}$ and the volume-dependent contribution $\vec{F}_\Omega^i$:

$$\vec{F}_p^i = \sum_{j=1}^{N_i} \vec{F}_{pair}^{ij} + \vec{F}_\Omega^i , \tag{2}$$

while the force $\vec{F}_\Omega^i$ in case of locally isotropic material can be calculated as:

$$\vec{F}_\Omega^i = -A_i \sum_{j=1}^{N_i} P_j S_{ij} \vec{n}_{ij} . \tag{3}$$

In Eq. (3) P_i is the pressure in the volume of the movable cellular automaton i, S_{ij} is the contact square between neighboring automata i and j, $\vec{n}_{ij}$ is the unit vector directed along the line goes through the centres of i and j, A_i is the proportionality factor, which belongs to the material of the automaton i and in common case can be differ from A_j.

The concept of the MCA method also involves the introduction of a new type of state, namely the state of a pair of automata which may be linked or unlinked. In short, the linked state indicates that the pair is part of a solid body and the unlinked state indicates that during sliding the automata may behave like a granular material. By using criteria for linked-unlinked switching in the framework of the MCA method it is possible to simulate such events in the contact area like the discontinuity formation and accumulation of damage, as well as processes connected with mass mixing, velocity accommodation and so on. In the present investigations the "fracture" criteria for linked-unlinked switch was defined as critical value of stress intensity in the interacting pair. So, when the calculated stress intensity in a linked pair reaches the fracture strength of the softer material (epoxy matrix in our case) this pair becomes unlinked. After coming into contact with another automaton the unlinked-linked-transition may take place. The latter switching criteria are

controlled by a normal flow stress. That means that an adjustable amount of plastic deformation of the softer constituent is taken as prerequisite for the binding of automata together thus forming an aggregate of linked particles.
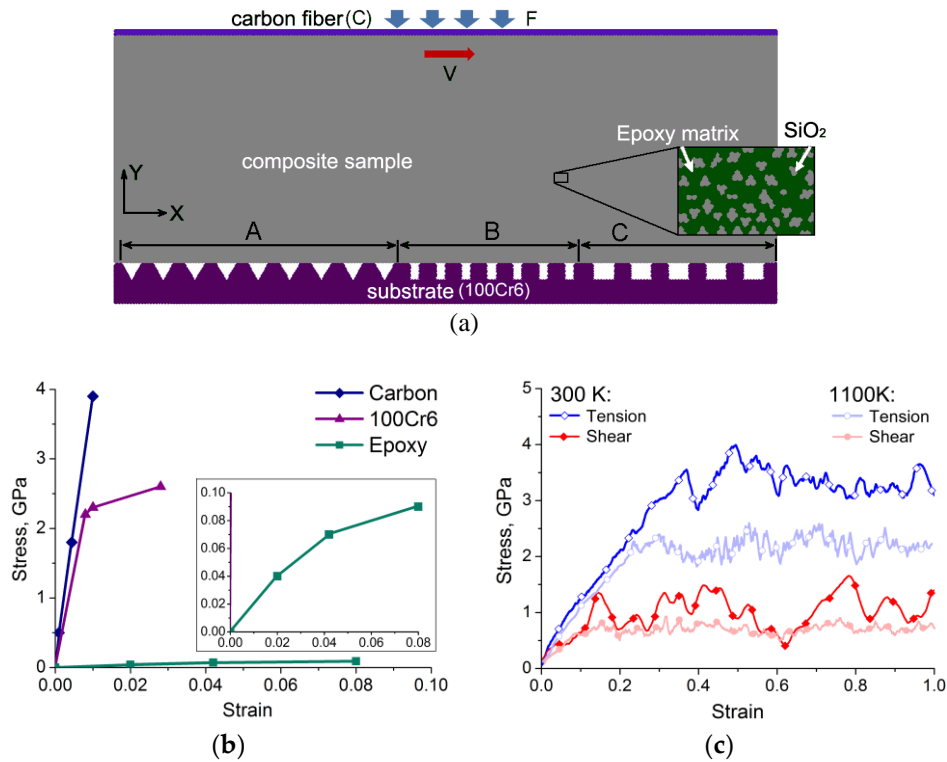
Fig. 1 (a) A general view of the simulated setup and a loading scheme. Details of the composite structure are shown by the inset. (b) Stress-strain diagrams for materials used in the model of a local contact of the hybrid NC. (c) Stress-strain curves of uniaxial tension and shear for silica nanoparticles at ambient and elevated temperatures calculated with use of molecular dynamics method.

Figure 1a shows the loading scheme and the initial structure of the simulated setup. The region under consideration includes the surface of unmovable rigid substrate created by automata with properties of 100Cr6 steel, as well as adjacent surface layers of the nanocomposite containing nanoinclusions. Two samples with two characteristic sizes of silica nanoinclusions (20 nm and 60 nm) were considered. The inclusions were implemented by movable cellular automata with the properties of silica and the automata of the matrix possessed the properties of epoxy. The diameter of each automaton was set equal to 10 nm, which corresponds to the average diameter of the smallest silica nanoparticles [18]. The geometry of the sample was 12 x 4 μm along the X and Y directions, respectively, and the total number of automata in the simulated setup was about 25 thousand. The evolution of an ensemble of movable cellular automata was defined by solution of the

system in Eq. (1) with the time step $\Delta t = 0.25\,\text{ps}$ [13]. The latter is not freely adjustable but depends on the size of automata and on their elastic properties like:

$$\Delta t < d\sqrt{\rho/E}\,, \tag{4}$$

where d is the automata diameter, ρ and E are the density and elastic modulus of each material uses in the setup.

The response functions used to describe the interaction between automata representing different materials are shown in Fig. 1b. They were built on the basis of existing experimental data [19-21]. Since in our preliminary studies [22] it was not possible to obtain the required response of the hybrid PNC with varying the pv-factor in the present model for silica particles, the temperature dependence of the mechanical properties calculated by the molecular dynamics method was introduced [23, 24]. Stress-strain diagrams for silica nanoparticles at conditions of ambient and elevated temperatures are shown in Figure 1c.

In order to study the relationship between the filler properties and microgeometry of the substrate surface, three regions "A", "B", and "C" with different characteristic surface profiles were designed in the counterbody as shown in Fig 1a. In region "A", the surface profile of the substrate was characterized by V-shaped grooves with a width of 70 nm at the base of the triangle. Region "B" of the counterbody profile contained rectangular recesses with a width of 40 nm, and region "C" included rectangular recesses of a surface profile with a width of 80 nm. The depth of all types of depressions was the same and equal to 70 nm. To analyze the effect of pv-factor on tribological properties of the hybrid polymer nanocomposite the surface profile of the counterbody was changed to flat, i.e. without additional grooves. This choice of the counterbody surface profile was motivated by the intention to speed-up the process in order to achieve the steady-state sliding regime, when the friction coefficient is localized at a certain value, and the position and thickness of the tribolayer are dynamically stabilized [25]. Moreover, as it was shown in [14, 25] the initial roughness profiles of the counterbody on the nanometer scale do not impact significantly on the value of the friction coefficient.

Loading conditions that simulate relative sliding under dry contact were implemented by additional action on the automata of the upper layer of the sample, which were characterized by the properties of carbon fibre. Thus the tangential (sliding) velocity (v) was applied to all automata of the upper layer as shown in Fig. 1a. Its value was varied in the range from 0.05 to 4 m/s in various tasks while maintaining the specified value throughout the calculating time. Simultaneously the additional normal forces (F) simulating a compression p = 30 MPa were set. Periodic boundary conditions were used to simulate the extension of the simulated fragment along the X axis. It was assumed that the surface layers initially did not contain any damages on the scale under consideration. Furthermore, absence of adhesive forces between the sample and the substrate material was assumed.

3. RESULTS OF SLIDING SIMULATION

3.1. The influence of nanofillers size

Figure 2a shows a fragment of the structure of a hybrid PNC filled by silica nanoparticles with the characteristic size of 20 nm at the steady-state sliding regime.

Rectangles in the figure indicate areas with different types of microgeometry of the counterbody surface. It can be seen that, regardless of the type of microgeometry ("A", "B" or "C"), in all types of depressions, there are automata that belong to both the matrix and the inclusion material. This is also well-seen in Fig. 2b, where the pairs of automata in the "linked" state are indicated by the segments between centers of two neighboring particles. At the steady-state of sliding, the automata with the matrix properties are mostly represented by single particles while in the area with microgeometry of type "C" the agglomerates of the epoxy still exist. Such a distribution of automata with properties of the matrix and SNP can be explained by the small size of the nanofiller particles and their ability to settle in all types of considered recesses.
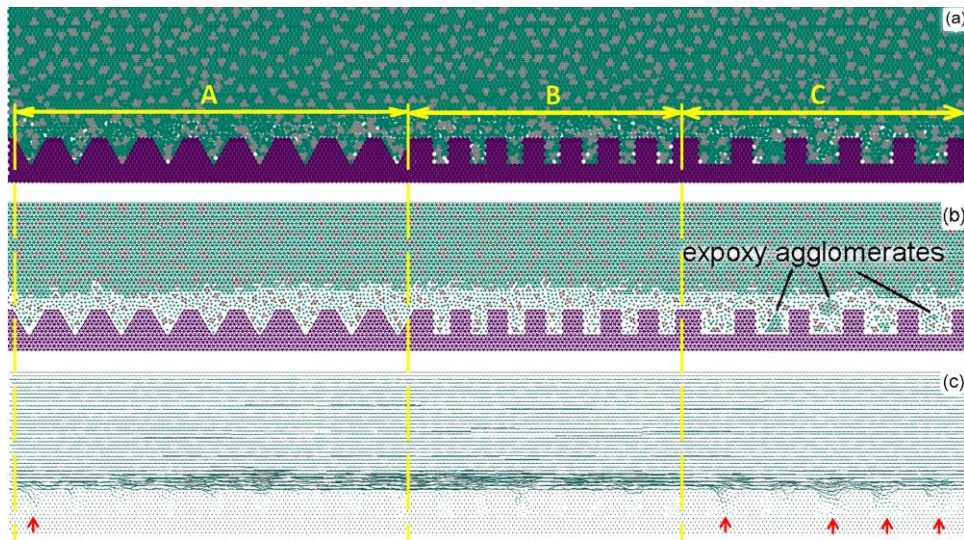
Fig. 2 The fragment of resulting structure (a) and structure of the inter-automata states (b) of a hybrid PNC with SNP 20 nm after ~10 μs of sliding. (c) Trajectories of automata for the considered fragment of the structure at the steady sliding in the time interval of $10 \div 30$ μs. Relative sliding velocity v = 1 m/s. Hereafter automata with the properties of epoxy are marked in green and with the properties of silica – in grey. Arrows indicate the non-zeros trajectories of automata in counterbody grooves.

Thus, in the case of a polymer-based hybrid nanocomposite with small nanofillers, the formation of a stable tribolayer from SNP will be hindered by the fact that SiO_2 particles will be mixed with epoxy, which will eventually be removed from the tribocontact area due to heating and evaporation. However, this factor determines the duration of the grinding-in stage before the system transfer to the regime of stable sliding with a low friction coefficient. The trajectories in Fig. 2c also confirm that the automata mobility remains localized in a narrow layer contacting with the substrate at steady-state friction. Changes in the automata positions inside the recesses of the counterbody profile are practically not observed. There is only a slight involvement of the particles from large depressions of the "C" region (shown by arrows).

Figure 3a shows a fragment of the structure of a polymer-based hybrid nanocomposite filled by SNP with the characteristic size of 60 nm at the steady-state sliding regime. In the case of the large size of the nanofiller particles, their filling of the recesses of region "B" of the counterbody profile is less frequently observed. This is explained by the proximity of the characteristic particle sizes of inclusions and the width of the recesses. Separate automata with the properties of silica, which can be seen inside depressions of the region "B", are fragments of larger particles that collapsed during sliding. Similar conclusions can be made for the region "A" of the counterbody surface profile. However, the patterns described above for this part of the substrate are less pronounced. At the same time, according to the structure of inter-automata states, shown in Fig. 3b, almost all depressions of the counterbody are covered with silica nanoparticles. This arrangement of SNP should facilitate the formation of a transfer tribofilm. This conclusion is also well confirmed by the automata trajectories at the steady-state sliding regime presented in Fig. 3c. The nonzero trajectories of automata are preserved only in the large grooves of the region "C", but there are fewer of them than in the sample with smaller SNP.
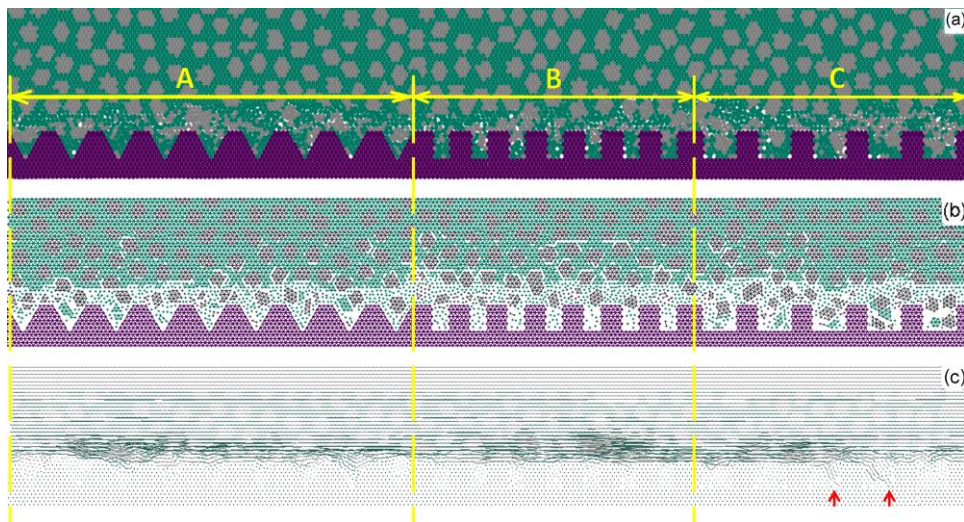
Fig. 3 The fragment of the resulting structure (a) and the structure of the inter-automata states (b) of a hybrid PNC with SNP 60nm after ~10 μs of sliding. (c) Trajectories of automata for the considered fragment of structure at the steady stage of sliding in the time interval of 10 ÷ 30 μs. Relative sliding velocity v = 1 m/s.

Thus, in the case of a hybrid PNC with a nanofiller particle comparable with the size of the counterbody surface grooves, the formation of a stable tribolayer from SNP will occur more intensively. Indeed, in this case, large SiO_2 particles remain localized in a narrow tribolayer, where intense frictional heating of the material occurs and there is a high probability of the transition of silica particles to a state similar to an amorphous one. As was shown in [23, 24], such a transition determines the regime of stable sliding with a low friction coefficient. The latter characterizes hybrid polymer nanocomposites.

3.2. The influence of sample geometry

To study the possible relationship between the geometry of the hybrid PNC and the thickness of the tribolayer two samples differing in size along the Y-axis (4 and 2 µm) were simulated. All other parameters of the system related to loading conditions, width, and the conterbody surface profile remained unchanged. According to the results, during the relative sliding, most automata remain in a "linked" state with their neighbors, which are depicted by the segments connecting the centers of such particles. However, in the immediate vicinity of the sample-conterbody interface, a layer of "unlinked" particles was formed, which is necessary to accommodate the velocities of the moving sample relative to the substrate. The thickness of the layer (h), in which the active movement of particles occurs, in the case of higher sample is about 10-12 times of the automata diameter while for a sample with a height of about 2 µm this value is limited to 6-7 diameters of the automata. Such a difference in values can be explained by the manifestation of different damping properties and stress conditions of both samples. Thus, the geometry of the sample affects the thickness of the formed tribofilm, including the layer of mechanical mixing of particles. An increase in the height of the sample leads to an increase in the thickness of the tribofilm (Fig. 4). It should be noted that the calculated average value of the friction coefficient for the simulated PNC sample turns out to be close to the experimentally observed value in the range of about $0.2 \div 0.3$.
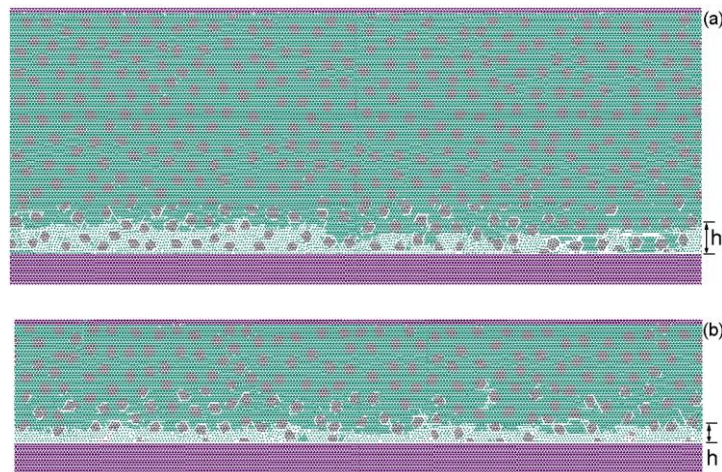
Fig. 4 The structures of inter-automata states after ~4 µs of sliding for the hybrid PNC samples with different size along the Y-axis: (a) 4 µm and (b) 2 µm. The shear strain in both cases is about 25%.

3.3. The effect of pv-factor

In order to study the influence of pv-factor on the tribological properties of a polymer-based hybrid nanocomposite the PNC sample with the geometry similar to one depicted in Fig. 4a was subjected to sliding loading with different conditions. Figure 5a shows the calculated values of the instantaneous and average friction coefficient for the system under consideration at different values of sliding velocity while maintaining the compression

conditions. The friction coefficient for the simulated system was calculated as the ratio between the normal and tangential forces. Averaging was performed over 100 adjacent instantaneous values of friction coefficient. It is well seen that with an increase of sliding velocity, and hence with an increase in the pv-factor, the friction coefficient for the simulated sample decreases. This is in good agreement with the experimental data, the values of which are depicted in Fig. 5b. For comparison the simulation results were shown as individual points, which were obtained by averaging friction coefficient values over the stage of steady-state sliding. Thus each point in the graph corresponds to individual plot shown in Fig. 5a. A similar slope for both the experimental and theoretical linear dependences is observed. The only difference is that the calculated data are shifted towards large values of pv-factor. This is due to the difference in values of applied compression. The high values of normal forces are easily explained by the small sizes of the model of a local contact spot of a hybrid PNC with a steel counterbody. Therefore, this difference can be interpreted as the difference between the nominal and actual compressive stresses. Otherwise, the presented dependence is in good agreement with the experimental data, which indicates the adequacy of the developed numerical model.
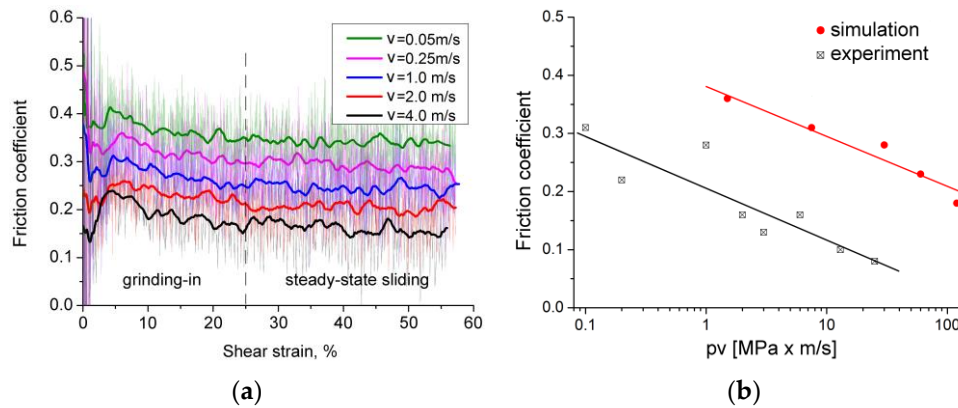
Fig. 5 (a) The instantaneous (thin lines) and average (bold curves) dependencies of friction coefficient for the hybrid PNC sample filled by SNP with the characteristic size of 60 nm at different values of relative sliding velocity. (b) Calculated and experimentally measured [11] data of friction coefficient vs. pv-factor, where solid lines are drawn according to the least squares method.

4. CONCLUSION

Based on the developed numerical model, the features of mechanical behavior of polymer-based hybrid nanocomposite at mesoscale levels under dry frictional contact were studied with explicit allowance for the microprofile of the counterbody surface and the characteristic sizes of nanofiller. Factors that contribute to the conditions for the formation of a stable tribofilm from silica nanoparticles are identified. According to the simulation results, the preferred nanofiller to ensure the improved friction properties of hybrid PNC is that, whose sizes are comparable to the characteristic size of the microprofile of the substrate surface. In this case, solid inclusions are localized in the near-surface area of the counterbody depressions

and the conditions necessary for the formation of an amorphized tribolayer from silica particles are created. It has been found that the V-shaped grooves of the recesses are preferable over the rectangular recesses of the substrate surface microprofile to ensure stable friction conditions. Calculations showed also that with an increase of pv-factor, the friction coefficient for the simulated sample decreases. This tendency is in good agreement with the available experimental data, which indicates the adequacy of the developed numerical model.

REFERENCES

1. Vaia, R.A., Wagner, H.D., 2004, *Framework for nanocomposites,* Materials Today, 7, pp. 32–37.
2. Kotsilkova, R., Silvestre, C., Cimmino, S., 2007, *Thermoset nanocomposites for engineering applications*, in: R. Kotsilkova (Ed.), *Thermoset nanocomposites for engineering applications*, Rapra Technology, Shawbury, UK, pp. 1–12.
3. Tauqeer Ali, H., Akrami, R., Fotouhi, S., Pashmforoush, F., Fragassa, C., Fotouhi, M., 2020, *Effect of the stacking sequence on the impact response of carbon-glass/epoxy hybrid composites*, Facta Universitatis-Series Mechanical Engineering, 18(1), pp. 69-77.
4. Zare, Y., Rhee, K.Y., 2020, *A modeling approach for young's modulus of interphase layers in polymer nanocomposites*, Physical Mesomechanics, 23(2), pp. 176–181.
5. Bahadur, S., Sunkara, C., 2005, *Effect of transfer film structure, composition and bonding on the tribological behavior of polyphenylene sulfide filled with nano particles of TiO2, ZnO, CuO and SiC,* Wear, 258(9), pp. 1411-1421.
6. Zhang, H., Zhang, Z., Friedrich, K., et al., 2006, *Property improvements of in situ epoxy nanocomposites with reduced interparticle distance at high nanosilica content*. Acta Materialia, 54(7), pp. 1833-1842.
7. Hernández-Vargas, M.L., Castillo-Pérez, R., Flores-Cedillo, O., Campillo-Illanes, B.F., 2021, *Modification of macromolecular dynamics in polyacrylic hybrid nanocomposite with un-treated SiO2 nanoparticles,* Materials Science and Engineering B, 265, 114976.
8. Ragosta, G., Abbate, M., Musto, P., et al., 2005, *Epoxy-silica particulate nanocomposites: Chemical interactions, reinforcement and fracture toughness,* Polymer, 46(23), pp. 10506-10516.
9. Zhang, L., Zhang, G., Chang, L., et al., 2016, *Distinct tribological mechanisms of silica nanoparticles in epoxy composites reinforced with carbon nanotubes, carbon fibers and glass fibers*, Tribology International, 104, pp. 225-236.
10. Zhang L., Qi H., Li G., et al., 2017, *Impact of reinforcing fillers' properties on transfer film structure and tribological performance of POM-based materials*, Tribology International, 109, pp. 58-68.
11. Zhang, G., Sebastian, R., Burkhart, T., Friedrich, K., 2012, *Role of monodispersed nanoparticles on the tribological behaviour of conventional epoxy composites filled with carbon fibers and graphite lubricants.* Wear, 292-293, pp. 176-187.
12. Zhang, G., Österle, W., Jim, B.C., Häusler, I., Hesse, R., Wetzel, B., 2016, *The role of surface topography in the evolving microstructure and functionality of tribofilms of an epoxy-based nanocomposite*, Wear, 364-365, pp. 48–56.
13. Dmitriev, A.I., Österle, W., Wetzel, B., 2015, *Mesoscale modeling of the mechanical and tribological behavior of a polymer matrix composite based on epoxy and 6vol.% silica nanoparticles*, Computational Materials Science, 110, pp. 204-214.
14. Dmitriev, A.I., Österle, 2010, *Modeling of brake pad-disc interface with emphasis to dynamics and deformation of structures*, Tribology International, 43(4), pp. 719-727.
15. Psakhie, S.G., Smolin, A.Yu., Shilko, E.V., et al., 1997, *About the Features of Transient to Steady State Deformation of Solids,* Journal of Materials Science and Technology, 13(1), pp. 69-72.
16. Czopor, J., Aniszewska, D., Rybaczuk, M., 2012, *The influence of defects on strength of ceramics modeled with Movable Cellular Automata,* Computational Materials Science, 51, pp. 151–155.
17. Shilko, E.V., Psakhie, S.G., Schmauder, S., Popov, V.L., Astafurov, S.V., Smolin, A.Yu., 2015, *Overcoming the limitations of distinct element method for multiscale modeling of materials with multimodal internal structure*, Computational Materials Science, 102, pp. 267–285.

18. Dmitriev, A.I., Häusler, I., Österle, W., 2016, *Modeling of the stress–strain behavior of an epoxy-based nanocomposite filled with silica nanoparticles*, Materials and Design, 89, pp. 950-956.
19. Basu, S., Moseson, A., Barsoum, M.W., 2006, *On the determination of spherical nanoindentation stress–strain curves*, Journal of Materials Research, 21, pp. 2628-2637.
20. Tinscher, R., Bahnsen C., Bomas H., et al., 2001, *Gefüge und mechanische Eigenschaften eines durch Sprühkompaktieren hergestellten Stahles 100Cr6,* Materialwissenschaft und Werkstofftechnik, 32, pp. 607-620.
21. Goggin, P.R., 1973, *The elastic constants of carbon-fibre composites*, Journal of Materials Science, 8(2), pp. 233-244.
22. Österle, W., Dmitriev, A.I., Gradt, T., et al., 2015, *Exploring the beneficial role of tribofilms formed from an epoxy-based hybrid nanocomposite,* Tribology International, 88, pp. 126-134.
23. Dmitriev, A.I., Nikonov, A.Yu., Österle, W., 2016, *MD Sliding simulations of amorphous tribofilms consisting of either SiO2 or carbon*, Lubricants, 4(3), pp. 1-24.
24. Dmitriev, A.I., Nikonov, A.Yu., Österle, W., 2018, *Molecular Dynamics Modeling of the Sliding Performance of an Amorphous Silica Nano-Layer - The Impact of Chosen Interatomic Potentials,* Lubricants, 6(2), pp. 43.
25. Dmitriev, A.I., Schargott, M., Popov, V.L., 2010, *Direct modelling of surface topography development in a micro-contact with the movable cellular automata method*, Wear, 268(7-8), pp. 877-885.